NASA Technical Paper 3311

March 1993

Green's Function Methods in Heavy Ion Shielding

John W. Wilson,
Robert C. Costen,
Judy L. Shinn,
and Francis F. Badavi

NASA

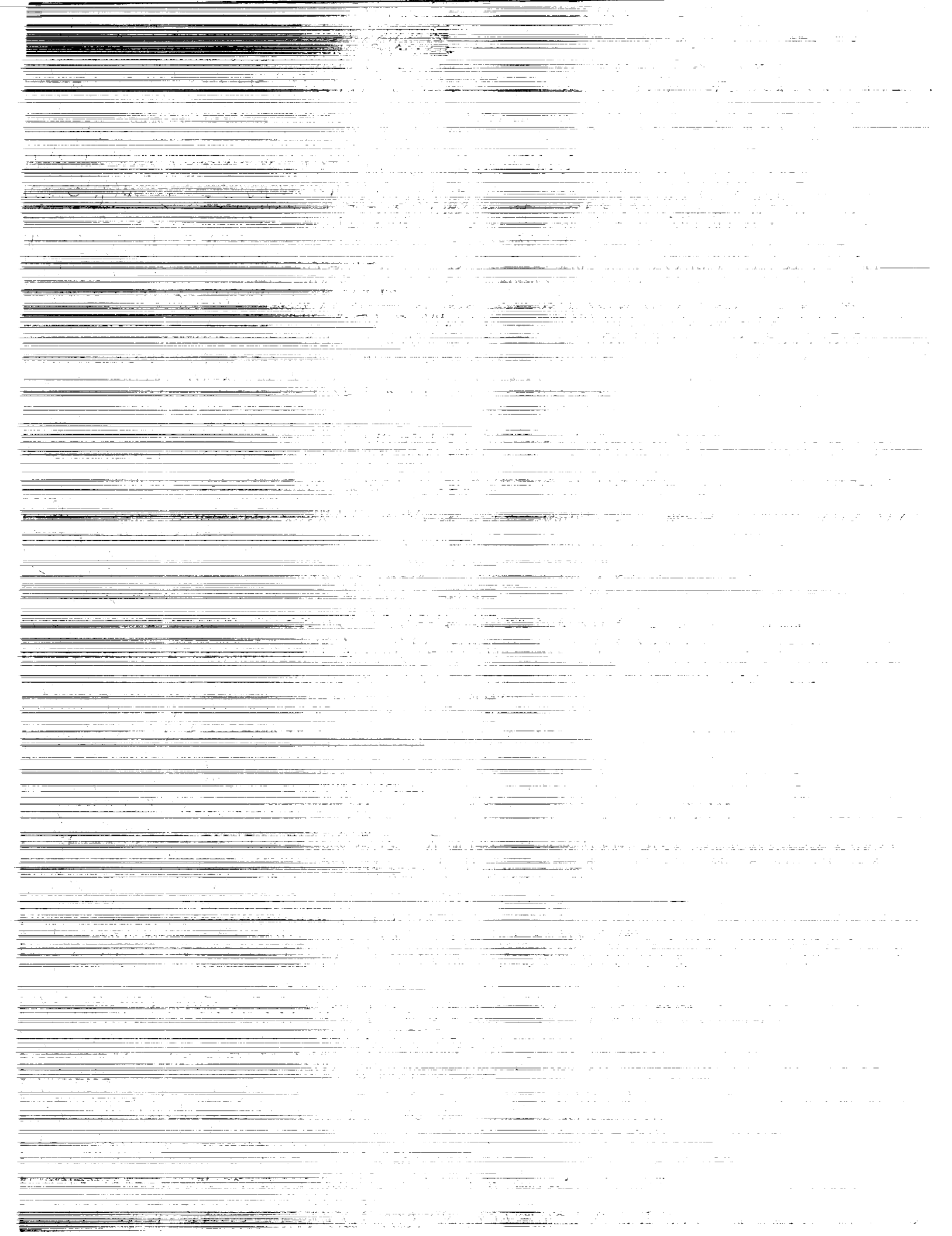

NASA Technical Paper 3311

1993

Green's Function Methods in Heavy Ion Shielding

John W. Wilson, Robert C. Costen, and Judy L. Shinn
Langley Research Center
Hampton, Virginia

Francis F. Badavi
Christopher Newport University
Newport News, Virginia

NASA
National Aeronautics and Space Administration
Office of Management
Scientific and Technical Information Program

Abstract

An analytic solution to the heavy ion transport equation in terms of Green's function is used to generate a highly efficient computer code for space applications. The efficiency of the computer code is accomplished by a nonperturbative technique extending Green's function over the solution domain. The computer code can also be applied to accelerator boundary conditions to allow code validation in laboratory experiments.

Introduction

From the inception of the Langley Research Center heavy ion shielding program (refs. 1–3), a close relationship has existed between code development and laboratory experiment (ref. 3). Indeed, the current goal is to provide computationally efficient high charge and energy (HZE) ion transport codes that can be validated with laboratory integral experiments and subsequently applied to space engineering design. In practice, two streams of code development (laboratory codes and engineering design codes) have prevailed because of the strong energy dependence of necessary atomic/molecular cross sections and the near singular nature of the boundary conditions of the laboratory beam (refs. 4–6).

The energy dependence of atomic/molecular cross sections is adequately dealt with by using the methods of Wilson and Lamkin (ref. 7) to develop efficient numerical procedures for space radiation (refs. 6 and 8–10). Although these codes can conceivably be applied to laboratory validation, methods to control truncation and discretization errors bear little resemblance to the space radiation codes that need validating. Thus, a radical reorientation is required to achieve the validation goals of the current LaRC heavy ion shielding program, and such an approach is presented in this paper by extending the work of Wilson and Badavi (ref. 11). This approach consists of a nonperturbative technique that allows highly accurate analytic solution over the solution domain of any practical problem. The following section presents a brief discussion of the fundamental transport equations and their formal solution.

Transport Theory

The transport equations are derived on the basis of conservation principles. Consider a region of space filled with matter described by appropriate atomic and nuclear cross sections. Sketch A shows a small portion of the region enclosed by a sphere of radius δ. The number of particles of type j leaving a surface element $\delta^2\ d\boldsymbol{\Omega}$ is given as $\phi_j(\mathbf{x}+\delta\boldsymbol{\Omega},\boldsymbol{\Omega},E)\delta^2\ d\boldsymbol{\Omega}$ where $\phi_j(\mathbf{x},\boldsymbol{\Omega},E)$ is the particle flux density, $\mathbf{x}$ is a vector to the center of the sphere, $\boldsymbol{\Omega}$ is normal to the surface element, and E is the particle energy. The projection of the surface element through the sphere center to the opposite side of the sphere defines a cylinder through which pass a number of particles of type j given as $\phi_j(\mathbf{x}-\delta\boldsymbol{\Omega},\boldsymbol{\Omega},E)\delta^2\ d\boldsymbol{\Omega}$. This number would equal the number of particles leaving the opposite face if the cylinder defined by the projection were a vacuum. The two numbers of particles in fact differ by the gains and the losses created by atomic and nuclear collisions as follows:

$$\begin{aligned}\phi_j(\mathbf{x}+\delta\boldsymbol{\Omega},\boldsymbol{\Omega},E)\delta^2\ d\boldsymbol{\Omega} = \phi_j(\mathbf{x}-\delta\boldsymbol{\Omega},\boldsymbol{\Omega},E)\delta^2\ d\boldsymbol{\Omega} \\ + \delta^2\ d\boldsymbol{\Omega}\int_{-\delta}^{\delta} dl \sum_k \int \sigma_{jk}(\boldsymbol{\Omega},\boldsymbol{\Omega}',E,E')\ \phi_k(\mathbf{x}+l\boldsymbol{\Omega},\boldsymbol{\Omega}',E')\ d\boldsymbol{\Omega}'\ dE' \\ - \delta^2\ d\boldsymbol{\Omega}\int_{-\delta}^{\delta} dl\ \sigma_j(E)\ \phi_j(\mathbf{x}+l\boldsymbol{\Omega},\boldsymbol{\Omega},E) \qquad (1)\end{aligned}$$

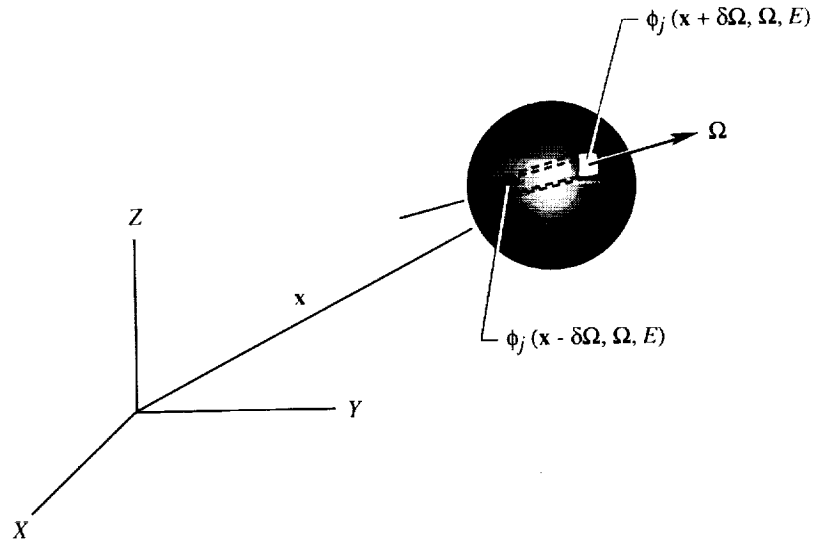

Sketch A

where $\sigma_j(E)$ and $\sigma_{jk}(\mathbf{\Omega}, \mathbf{\Omega}', E, E')$ are the media macroscopic cross sections. The cross section $\sigma_{jk}(\mathbf{\Omega}, \mathbf{\Omega}', E, E')$ represents all those processes by which type k particles moving in direction $\mathbf{\Omega}'$ with energy E' produce a type j particle in direction $\mathbf{\Omega}$ with energy E. Note, several reactions can accomplish this result, however, the appropriate cross sections of equation (1) are the inclusive ones. The second term on the right side of equation (1) is the source of secondary particles integrated over the total volume $2\delta(\delta^2\ d\mathbf{\Omega})$, and the third term is the loss through nuclear reaction integrated over the same volume. We expand the terms of each side as a Taylor series and retain terms to order δ^3 explicitly as

$$\begin{aligned}\delta^2\ d\mathbf{\Omega}\left[\phi_j(\mathbf{x},\mathbf{\Omega},E) + \delta\mathbf{\Omega}\cdot\nabla\phi_j(\mathbf{x},\mathbf{\Omega},E)\right] = \delta^2\ d\mathbf{\Omega}\,[\phi_j(\mathbf{x},\mathbf{\Omega},E) &- \delta\mathbf{\Omega}\cdot\nabla\phi_j(\mathbf{x},\mathbf{\Omega},E) \\ &+ 2\delta\sum_k\int\sigma_{jk}(\mathbf{\Omega},\mathbf{\Omega}',E,E')\ \phi_k(\mathbf{x},\mathbf{\Omega}',E')\ d\mathbf{\Omega}'\ dE' \\ &- 2\delta\sigma_j(E)\ \phi_j(\mathbf{x},\mathbf{\Omega},E)] + O(\delta^4) \qquad (2)\end{aligned}$$

This equation can then be divided by the cylindrical volume $2\delta(\delta^2\ d\mathbf{\Omega})$ and written as

$$\begin{aligned}\mathbf{\Omega}\cdot\nabla\phi_j(\mathbf{x},\mathbf{\Omega},E) = \sum_k\int\sigma_{jk}(\mathbf{\Omega},\mathbf{\Omega}',E,E')\ \phi_k(\mathbf{x},\mathbf{\Omega}',E')\ d\mathbf{\Omega}'\ dE' \\ - \sigma_j(E)\ \phi_j(\mathbf{x},\mathbf{\Omega},E) + O(\delta) \qquad (3)\end{aligned}$$

for which the last term $O(\delta)$ approaches zero in the limit as $\delta \to 0$. Equation (3) is recognized as a time-independent form of the Boltzmann equation for a tenuous gas. Atomic collisions (i.e., collisions with atomic electrons) preserve the identity of the particle, and two terms on the right side of equation (3) contribute to the gains and losses. The differential cross sections have the following approximate form for atomic processes:

$$\sigma^{at}_{jk}(\mathbf{\Omega},\mathbf{\Omega}',E,E') = \sum_n\ \sigma^{at}_{jn}(E')\ \delta(\mathbf{\Omega}\cdot\mathbf{\Omega}' - 1)\ \delta_{jk}\ \delta(E + \epsilon_n - E') \qquad (4)$$

where the superscript at represents atomic, n labels the electronic excitation levels, and ϵ_n represents the corresponding excitation energies, which are small (1–100 eV in most cases) compared with the

particle energy E. The atomic terms can then be written as

$$\sum_k \int \sigma_{jk}^{at}(\mathbf{\Omega}, \mathbf{\Omega}', E, E')\ \phi_k(\mathbf{x}, \mathbf{\Omega}', E')\ d\mathbf{\Omega}'\ dE' - \sigma_j^{at}(E)\ \phi_j(\mathbf{x}, \mathbf{\Omega}, E)$$

$$= \sum_n\ \sigma_{jn}^{at}(E + \epsilon_n)\ \phi_j(\mathbf{x}, \mathbf{\Omega}, E + \epsilon_n) - \sigma_j^{at}(E)\ \phi_j(\mathbf{x}, \mathbf{\Omega}, E)$$

$$\approx \sum_n\ \sigma_{jn}^{at}(E)\ \phi_j(\mathbf{x}, \mathbf{\Omega}, E) + \sum_n\ \epsilon_n\ \frac{\partial}{\partial E}\left[\sigma_{jn}^{at}(E)\ \phi_j(\mathbf{x}, \mathbf{\Omega}, E)\right] - \sigma_j^{at}(E)\ \phi_j(\mathbf{x}, \mathbf{\Omega}, E)$$

$$= \frac{\partial}{\partial E}\ S_j(E)\ \phi_j(\mathbf{x}, \mathbf{\Omega}, E) \tag{5}$$

because the stopping power is

$$S_j(E) = \sum_n\ \sigma_{jn}^{at}(E)\epsilon_n \tag{6}$$

and the total atomic cross section is

$$\sigma_j^{at}(E) = \sum_n\ \sigma_{jn}^{at}(E) \tag{7}$$

Equations (5) to (7) allow us to rewrite equation (3) in the usual continuous slowing down approximation as

$$\left[\mathbf{\Omega} \cdot \nabla - \frac{\partial}{\partial E}\ S_j(E) + \sigma_j(E)\right]\ \phi_j(\mathbf{x}, \mathbf{\Omega}, E) = \int \sum_k \sigma_{jk}(\mathbf{\Omega}, \mathbf{\Omega}', E, E')\ \phi_k(\mathbf{x}, \mathbf{\Omega}', E')\ d\mathbf{\Omega}'\ dE' \tag{8}$$

where the cross sections of equation (8) now contain only the nuclear contributions. For convenience, we can rewrite this equation as the following matrix equation:

$$\mathbf{B}\boldsymbol{\phi} = \mathbf{P}\boldsymbol{\phi} \tag{9}$$

where $\mathbf{B}$ is a diagonal differential matrix operator consisting of the drift term, energy loss term, and collisional loss term on the left side of equation (8); $\boldsymbol{\phi}$ is a vector of the particle fields with the heaviest particles in the lowest entries; and $\mathbf{P}$ is the collisional source matrix that is assumed to be an upper triangular integral operator.

Equation (9) may be rewritten as

$$\boldsymbol{\phi} = \boldsymbol{\phi}_o + \mathbf{B}^{-1}\mathbf{P}\boldsymbol{\phi} \tag{10}$$

where $\boldsymbol{\phi}_o$ is the solution of the homogeneous equation and is equal to the incoming flux at the boundary. A propagation matrix Green's function $\mathbf{G}_o$, which is the inverse of the multivariate integrating factor (ref. 3) for the right side of equation (9), is defined as follows:

$$\boldsymbol{\phi} = \mathbf{G}_o\boldsymbol{\phi}_B + \mathbf{B}^{-1}\mathbf{P}\boldsymbol{\phi} \tag{11}$$

where $\boldsymbol{\phi}_B$ is the boundary condition and

$$\mathbf{B}\mathbf{G}_o = 0 \tag{12}$$

The Neumann series solution of equation (11) can then be written as

$$\boldsymbol{\phi} = \mathbf{G}_o\ \boldsymbol{\phi}_B + \mathbf{B}^{-1}\mathbf{P}\ \mathbf{G}_o\ \boldsymbol{\phi}_B + \mathbf{B}^{-1}\mathbf{P}\ \mathbf{B}^{-1}\mathbf{P}\ \mathbf{G}_o\ \boldsymbol{\phi}_B + \ldots \tag{13}$$

The series converges after N terms where N is the rank of the space because $\mathbf{B}^{-1}\mathbf{P}\,\mathbf{G}_o$ is a contraction mapping operator which is upper triangular (ref. 2). The complete Green's function is defined as

$$\phi = \mathbf{G}\phi_B \tag{14}$$

and is given by the series

$$\mathbf{G} = \mathbf{G}_o + \mathbf{B}^{-1}\mathbf{P}\,\mathbf{G}_o + \mathbf{B}^{-1}\mathbf{P}\,\mathbf{B}^{-1}\mathbf{P}\,\mathbf{G}_o + \ldots \tag{15}$$

and satisfies

$$\mathbf{G} = \mathbf{G}_o + \mathbf{B}^{-1}\mathbf{P}\mathbf{G} \tag{16}$$

where $\mathbf{B}^{-1}\mathbf{P}$ is factored from all but the first term on the right side of equation (15). Clearly, $\mathbf{G}$ satisfies the same operation equation as ϕ in equation (9). Thus,

$$\mathbf{B}\mathbf{G} = \mathbf{P}\mathbf{G} \tag{17}$$

where $\mathbf{G}$ is a matrix operator that reduces to the identity at all points on the boundary. In component form, equation (17) is written as follows:

$$\left[\mathbf{\Omega}\cdot\nabla - \frac{\partial}{\partial E}\,\widetilde{S}_j(E) + \sigma_j\right] G_{jm}(E, E_o, \mathbf{\Omega}, \mathbf{x}) = \sum_k \int \sigma_{jk}(E, E', \mathbf{\Omega}, \mathbf{\Omega}')\; G_{km}(E', E_o, \mathbf{\Omega}', \mathbf{x})\; d\mathbf{\Omega}'\; dE' \tag{18}$$

where $\widetilde{S}_j(E)$ is the change in E per unit distance, and E now denotes the energy per nucleon. An arbitrary solution to the Boltzmann equation within a closed convex region can be written as

$$\phi_j(E, \mathbf{\Omega}, \mathbf{x}) = \sum_m \int G_{jm}(E, E', \mathbf{\Omega} - \mathbf{\Omega}', \mathbf{x} - \mathbf{\Gamma}) \times f_m(E', \mathbf{\Omega}', \mathbf{\Gamma})\; d\mathbf{\Omega}'\; dE'\; d\mathbf{\Gamma} \tag{19}$$

where $f_m(E', \mathbf{\Omega}', \mathbf{\Gamma})$ is the incident flux at the boundary (ref. 12). Because the transport problem is formulated in terms of a single Green's function algorithm, the validation of the Green's function in the laboratory meets our objective of having a space-validated code (refs. 13 and 14).

The first step is to develop an equivalent Green's function algorithm in one dimension that matches our current capability in space radiation shielding (refs. 6 and 15). The algorithm is based on the closed-form solution to the following one-dimensional equation for a monoenergetic beam at the boundary:

$$\left(\frac{\partial}{\partial x} - \frac{\partial}{\partial E}\,\widetilde{S}_j(E) + \sigma_j\right) G_{km}(E, E_o, x) = \sum_k \int \sigma_{jk}(E, E')\; G_{km}\,(E', E_o, x)\; dE' \tag{20}$$

The possibility of validation for ^{20}Ne beams of this algorithm (with multiple scattering corrections) has already shown promise (refs. 5 and 16), but improvements in the nuclear data base are required to achieve agreement. If we restrict our considerations to multiple charged ions, then the right side of equation (20) can be further reduced to

$$\left[\frac{\partial}{\partial x} - \frac{\partial}{\partial E}\,\widetilde{S}_j(E) + \sigma_j\right] G_{jm}(E, E_o, x) = \sum_k \sigma_{jk}\; G_{km}(E, E_o, x) \tag{21}$$

for which we now consider the solution.

Approximate Green's Function

We now derive an approximate Green's function from equation (21), which can be simplified by transforming the energy into the residual range as

$$r_j = \int_0^E \frac{dE'}{\widetilde{S}_j(E')} \tag{22}$$

and defining new field variables as

$$\psi_j(x, r_j) = \widetilde{S}_j(E)\ \phi_j(x, E) \tag{23}$$

$$\mathcal{G}_{jm}(x, r_j, r'_m) = \widetilde{S}_j(E)\ \mathrm{G}_{jm}(x, E, E') \tag{24}$$

so that equation (21) becomes

$$\left(\frac{\partial}{\partial x} - \frac{\partial}{\partial r_j} + \sigma_j\right) \mathcal{G}_{jm}(x, r_j, r'_m) = \sum_k \frac{\nu_j}{\nu_k} \sigma_{jk}\ \mathcal{G}_{km}(x, r_j, r'_m) \tag{25}$$

where ν_j is the range scaling parameter, $\nu_j = Z_j^2/A_j$. The boundary condition for the Green's function is

$$\mathcal{G}_{jm}(0, r_j, r'_m) = \delta_{jm}\ \delta(r_j - r'_m) \tag{26}$$

and the full solution for an arbitrary boundary condition is

$$\psi_j(x, r_j) = \sum_m \int_0^\infty \mathcal{G}_{jm}(x, r_j, r'_m)\ f_m(r'_m)\ dr'_m \tag{27}$$

The solution to equation (25) can be written as a perturbation series as

$$\mathcal{G}_{jm}(x, r_j, r'_m) = \sum_i \mathcal{G}^{(i)}_{jm}(x, r_j, r'_m) \tag{28}$$

where

$$\mathcal{G}^{(0)}_{jm}(x, r_j, r'_m) = g(j)\ \delta_{jm}\ \delta(x + r_j - r'_m) \tag{29}$$

and

$$\mathcal{G}^{(1)}_{jm}(x, r_j, r'_m) \approx \frac{\nu_j\ \sigma_{jm}\ g(j, m)}{x(\nu_m - \nu_j)} \tag{30}$$

where $\mathcal{G}^{(1)}_{jm}(x, r_j, r'_m)$ is zero unless

$$\frac{\nu_j}{\nu_m}(r_j + x) \le r'_m \le \frac{\nu_j}{\nu_m}\ r_j + x \tag{31}$$

The second-order term is

$$\mathcal{G}^{(2)}_{jm}(x, r_j, r'_m) \approx \sum_k \frac{\sigma_{jk}\ \sigma_{km}\ g(j, k, m)}{r'_{ju} - r'_{j\ell}} \tag{32}$$

and is nonzero for

$$r'_{m\ell} \le r'_m \le r'_{mu} \tag{33}$$

where

$$r'_{mu} = \left\{ \begin{array}{ll} \frac{\nu_j}{\nu_m} r_j + x & (\nu_m > \nu_k > \nu_j) \\ \frac{\nu_j r_j + \nu_k x}{\nu_m} & (\nu_k > \nu_m > \nu_j) \\ \frac{\nu_j}{\nu_m} r_j + x & (\nu_m > \nu_j > \nu_k) \end{array} \right\} \tag{34}$$

and

$$r'_{m\ell} = \left\{ \begin{array}{ll} \frac{\nu_j}{\nu_m} (r_j + x) & (\nu_m > \nu_k > \nu_j) \\ \frac{\nu_j}{\nu_m} (r_j + x) & (\nu_k > \nu_m > \nu_j) \\ \frac{\nu_j r_j + \nu_k x}{\nu_m} & (\nu_m > \nu_j > \nu_k) \end{array} \right\} \tag{35}$$

and r'_{ju} and $r'_{j\ell}$ are found at the limits of equations (34) and (35). The third-order term is

$$\mathcal{G}^{(3)}_{jm}(x, r_j, r'_m) \approx \sum_{k,\ell} \frac{\sigma_{jk}\ \sigma_{k\ell}\ \sigma_{\ell m}\ g(j,k,\ell,m)}{r'_{ju} - r'_{j\ell}} \tag{36}$$

Higher order terms are similarly derived. In equation (36), the function g of n arguments are given by

$$g(j) = \exp(-\sigma_j\ x) \tag{37}$$

and

$$g(j_1, j_2, \ldots, j_n, j_{n+1}) = \frac{g(j_1, j_2, \ldots, j_{n-1}, j_n) - g(j_1, j_2, \ldots, j_{n-1}, j_{n+1})}{\sigma_{j_{n+1}} - \sigma_{j_n}} \tag{38}$$

As noted in reference 11, the solution to equation (21) can be written in terms of equation (38) as follows:

$$\psi_j(x, r_j) = \exp(-\sigma_j x) f_j(r_j + x) + \sum_{m,i} \mathcal{G}^{(i)}_{jm}(x) \left\{ F_m(r'_{mu}) - F_m(r'_{m\ell}) \right\} \tag{39}$$

where

$$\mathcal{G}^{(i)}_{jm}(x) = \sum_{j_1, j_2, \ldots, j_{n-2}} \frac{\sigma_{jj_1}\sigma_{j_1 j_2}, \ldots, \sigma_{j_{n-2}m}\ g(j, j_1 j_2, \ldots, j_{n-2}, m)}{\Delta^{(i)}} \tag{40}$$

for $(i = 1)$

$$\Delta^{(1)} = x \left(\frac{\nu_m}{\nu_j} - 1 \right) \tag{41}$$

and for $(i > 1)$

$$\Delta^{(i)} = \left\{ \begin{array}{ll} x \left(\frac{\nu_m}{\nu_j} - 1 \right) & (\nu_m > \nu_k > \nu_j) \\ x \left(\frac{\nu_k}{\nu_j} - 1 \right) & (\nu_k > \nu_m > \nu_j) \\ x \left(\frac{\nu_m}{\nu_j} - \frac{\nu_k}{\nu_j} \right) & (\nu_m > \nu_j > \nu_k) \end{array} \right\} \tag{42}$$

In equation (39), $F_m(r)$ is the integral flux at the boundary and can be represented as

$$F_m(r) = \int_r^\infty f_m(r')\ dr' \tag{43}$$

Implementation of equation (39) can now be accomplished independent of the character of the boundary values $f_m(r')$ to give accurate results for both space and laboratory applications.

Results of Perturbation Series

The solutions given in equations (23) to (43) contain a finite number of terms, but higher terms contain large numbers of components. Thus, only a few terms are usually generated. To better understand the nature of the solutions given by equations (30), (32), and (36), we now examine the perturbation series approximation to the scaled Green's function for a broad set of fragments. Figure 1 shows the first three collisional contributions to the Green's function for producing ^{52}Cr. In the figure, the atomic weight of each projectile (A_p) is truncated to the nearest isotope. The main contribution comes from near projectile elements up to third collision terms. Figure 2 shows the relative contribution of each term. The third collision term contributes less than 20 percent over the domain, and the contributions of higher order terms are smaller. Although fourth collision terms are not negligible at 50 cm, the total ^{52}Cr production at this depth is small. (See fig. 3.)

Figures 4 to 6 show similar results for ^{40}Ar production. The importance of the higher order terms in producing the lighter fragment is apparent when figure 2 is compared with figure 5. For example, the third collision for ^{40}Ar is as large as 40 percent in the displayed domain. Figures 7 to 9 show the ^{28}Si production terms. The third-order ^{28}Si production term dominates at large depths, and higher order terms are expected to be large. The main ^{28}Si production comes from collision with primary ions up to mass 42. Figures 10 to 12 show similar results for ^{16}O production. Clearly, terms of fourth and higher orders must be added into any meaningful calculation, but such terms require lengthy computational procedures. To evaluate the Green's function to all orders of collisions, we now derive a nonperturbative procedure. Thus, convergence problems associated with the calculations described in this section are circumvented.

Nonperturbative Procedures

In generating the graphs in figures 1 to 12, we found that the large number of terms contributing at large depths leads to an inefficient computational procedure. One of the difficulties is that many isotopes can be produced in successive collisions of the incident ions and their collision products. The first three terms of equation (28) are evaluated rather rapidly; thus, one question remains. How are the higher order terms to be made efficient? The following example is one possible approach.

The generator equation of the g-functions is given as a solution to the following equation:

$$\left[\frac{d}{dx} + \sigma_j\right] g_{jm}(x) = \sum_k \sigma_{jk}\, g_{km}(x) \tag{44}$$

This equation is subject to the boundary condition $g_{jm}(0) = \delta_{jm}$. Thus, it can be inverted as

$$g_{jm}(x) = \delta_{jm}\, \exp(-\sigma_j x) + \int_0^x \sum_k \sigma_{jk}\, \exp[-\sigma_j(x-y)]\, g_{km}(y)\, dy \tag{45}$$

where m denotes the solution for incident ion type m at the boundary ($x = 0$). Assume the solution of this equation is

$$g_{jm}^{(0)}(x) = \delta_{jm}\, \exp(-\sigma_j x) \tag{46}$$

and the iterated equation is

$$g_{jm}^{(i)}(x) = \int_0^x \sum_k \sigma_{jk}\, \exp[-\sigma_j(x-y)]\, g_{km}^{(i-1)}(y)\, dy \tag{47}$$

The higher order terms can be summed as

$$\sum_{i\geq 2} g_{jm}^{(i)}(x) = \int_0^x \sum_k \sigma_{jk} \exp\left[-\sigma_j(x-y)\right] \left[g_{km}^{(1)}(y) + \sum_{i\geq 2} g_{km}^{(i)}(y)\right] dy$$
$$= g_{jm}^{(2)}(x) + \int_0^x \sum_k \sigma_{ik} \exp\left[-\sigma_j(x-y)\right] \sum_{i\geq 2} g_{km}^{(i)}(y)\, dy \tag{48}$$

We find the following relation for the full series:

$$g_{jm}(x) = \sum_k g_{jk}(x-y)\, g_{km}(y) \tag{49}$$

The appendix contains a derivative of this equation. Note that just as $g_{jm}(x)$ is the solution of equation (44) with $g_{jm}(0) = \delta_{jm}$, $g_{jm}(x)$ is the solution of equation (44) having the value $g_{jm}(y)$ at $x = y$. Equation (49) can be used to generate solutions to all orders and arbitrary depths. Because equation (49) is an algebraic relationship that is true for an arbitrary y, we expect a rapid evaluation to arbitrary order and highly efficient computations, especially on vector processors. It follows from equations (29), (30), (32), (36), and (40) that the full Green's function can be written as

$$\mathcal{G}_{jm}(x, r_j, r'_m) = \exp(-\sigma_j x)\, \delta_{jm}\, \delta(x + r_j - r'_m) + \frac{\sigma_{jm}}{\Delta^{(1)}}\, g(j,m) + \frac{g_{jm}(x) - g(j)\, \delta_{jm} - \sigma_{jm}\, g(j,m)}{\Delta^{(2)}} \tag{50}$$

where the domains of successive terms are given by equations (31) and (33). Equation (50) can now be used to generate solutions to the ion transport problem.

A practical computation consists of three steps. The first step is to use the recurrence relation in equation (49) to adequately cover the solution domain with $g_{jm}(x)$. The second step is to evaluate the differential and integral spectra at the boundary by equation (43), and the third step is to use the following equation to evaluate the solution over the domain:

$$\psi_j(x, r_j) = \exp(-\sigma_j x) f_j(r_j + x) + \sum_m \frac{\sigma_{jm}\, g(j,m)}{\Delta^{(1)}} \left[F_m(r'_{mu}) - F_m(r'_{m\ell})\right]$$
$$+ \sum_{m,k} \frac{g_{jkm}(x) - g(j)\delta_{jm} - \sigma_{jm}\, g(j,m)}{\Delta^{(2)}} \left[F_m(r'_{mu}) - F_m(r'_{m\ell})\right] \tag{51}$$

where r'_{mu} and $r'_{m\ell}$ in the second term are given by the inequality limits of equation (33), and r'_{mu} and $r'_{m\ell}$ in the third term are given by equations (34) and (35). The quantity denoted as $g_{jkm}(x)$ is given as

$$g_{jkm}(x) = g_{jk}(x-y) g_{km}(y) \tag{52}$$

These nonperturbative techniques hold great promise for accurate and efficient computational methods for evaluation of the HZE particle fields in space and laboratory problems. However, the techniques must still be extended to light ion and especially neutron fields.

Results of Nonperturbative Procedures

A computer program has been written to calculate the Green's function with these nonperturbative methods. Figure 13 shows the values for the collision related terms of $\mathcal{G}_{jm}(x, r_j, r'_m)$. In the figure, x is the depth in a water medium, and Z_p is the charge of the incident projectile. Specifically produced species are noted in the figure. The production of any given species is dominated by the projectiles of nearly the same but greater charge. Figure 14 shows the relative contribution

of the first collision term. The multiple collision terms are more important for those projectiles whose charge is far removed from the specific species. For example, the first collision term contributes $\approx$20 percent to the ^{16}O flux at 50 cm for Ni ions ($A_P = 59$) to a third-order approximation (fig. 11(a)); however, it only contributes about 10 percent to the O flux when all orders are considered (fig. 14). The Green's function and equation (51) are used to evaluate the composition of a monoenergetic 535 MeV/nucleon Fe beam in a water column at several depths; figure 15 shows the results. These results will be compared with other results from experiments in the near future. The greatest advantage of the nonperturbative method is the computation efficiency. For example, to complete the computation for figures 1 to 12 required a week of time on a Digital Equipment Corp. VAX 785 compared with a few minutes to complete the computations for figures 13 to 15.

Concluding Remarks

The Green's function is a consistent method for developing space shielding codes that can be validated in laboratory experiments. Perturbation theory is a means of generating the Green's function for such purposes, but it is hampered by the inefficiency of the computational procedures. A nonperturbative technique is derived in which high computational efficiency is achieved without loss of accuracy. These nonperturbative methods hold great promise in allowing highly efficient computer codes for space shielding. The computer code can also be applied to accelerator boundary conditions to allow code validation in laboratory experiments.

NASA Langley Research Center
Hampton, VA 23681-0001
January 22, 1993

Appendix

A Derivation of Equation (49)

The generator equation (44) for $g_{jm}(x)$ has the same form and boundary conditions as the Green's function equation (17). The corresponding particle fluence equation (9) is given by

$$\left(\frac{d}{dx} + \sigma_j\right)\ \phi_j(x) = \sum_k \sigma_{jk}\ \phi_k(x) \tag{A1}$$

where $\phi_k(0)$ is known, and the Green's function solution (14) is given by

$$\phi_j(x) = \sum_m\ g_{jm}(x)\ \phi_m(0) \tag{A2}$$

We also have

$$\phi_k(y) = \sum_m\ g_{km}(y)\ \phi_m(0) \tag{A3}$$

where y denotes a point on the X-axis.

For $x > y$, we can also write

$$\phi_j(x) = \sum_k\ g_{jk}(x-y)\ \phi_k(y) \tag{A4}$$

Substituting equation (A3) into equation (A4) gives

$$\phi_j(x) = \sum_m \sum_k\ g_{jk}(x-y)\ g_{km}(y)\ \phi_m(0) \tag{A5}$$

By comparing this equation with equation (A2), we obtain the result

$$g_{jm}(x) = \sum_k\ g_{jk}(x-y)\ g_{km}(y)$$

which is equation (49).

References

1. Wilson, John W.; and Costner, Christopher M.: *Nucleon and Heavy-Ion Total and Absorption Cross Section for Selected Nuclei.* NASA TN D-8107, 1975.

2. Wilson, John W.: *Analysis of the Theory of High-Energy Ion Transport.* NASA TN D-8381, 1977.

3. Wilson, J. W.: Depth-Dose Relations for Heavy Ion Beams. *Virginia J. Sci.,* vol. 28, no. 3, 1977, pp. 136–138.

4. Wilson, John W.: *Heavy Ion Transport in the Straight Ahead Approximation.* NASA TP-2178, 1983.

5. Wilson, John W.; Townsend, L. W.; Bidasaria, H. B.; Schimmerling, Walter; Wong, Mervyn; and Howard, Jerry: ^{20}Ne Depth-Dose Relations in Water. *Health Phys.,* vol. 46, no. 5, May 1984, pp. 1101–1111.

6. Wilson, John W.; and Badavi, F. F.: Methods of Galactic Heavy Ion Transport. *Radiat. Res.,* vol. 108, 1986, pp. 231–237.

7. Wilson, John W.; and Lamkin, Stanley L.: Perturbation Theory for Charged-Particle Transport in One Dimension. *Nucl. Sci. & Eng.,* vol. 57, no. 4, Aug. 1975, pp. 292–299.

8. Wilson, John W.; Townsend, Lawrence W.; Nealy, John E.; Chun, Sang Y.; Hong, B. S.; Buck, Warren W.; Lamkin, S. L.; Ganapol, Barry D.; Khan, Ferdous; and Cucinotta, Francis A.: *BRYNTRN: A Baryon Transport Model.* NASA TP-2887, 1989.

9. Shinn, Judy L.; Wilson, John W.; Weyland, Mark; and Cucinotta, Francis A.: *Improvements in Computational Accuracy of BRYNTRN (A Baryon Transport Code).* NASA TP-3093, 1991.

10. Shinn, Judy L.; and Wilson, John W.: *An Efficient HZETRN (A Galactic Cosmic Ray Transport Code).* NASA TP-3147, 1992.

11. Wilson, J. W.; and Badavi, F. F.: New Directions in Heavy Ion Shielding. *Proceedings of the Topical Meeting on New Horizons in Radiation Protection and Shielding,* American Nuclear Soc., Inc., 1992, pp. 205–211.

12. Wilson, John W.; and Khandelwal, G. S.: Proton Dose Approximation in Arbitrary Convex Geometry. *Nucl. Technol.,* vol. 23, no. 3, Sept. 1974, pp. 298–305.

13. Wilson, John W.; Lamkin, Stanley L.; Farhat, Hamidullah; Ganapol, Barry D.; and Townsend, Lawrence W.: *A Hierarchy of Transport Approximations for High Energy Heavy (HZE) Ions.* NASA TM-4118, 1989.

14. Wilson, J. W.; Townsend, L. W.; Lamkin, S. L.; and Ganapol, B. D.: A Closed-Form Solution to HZE Propagation. *Radiat. Res.,* vol. 122, no. 3, June 1990, pp. 223–228.

15. Wilson, John W.; Chun, Sang Y.; Badavi, Forooz F.; Townsend, Lawrence W.; and Lamkin, Stanley L.: *HZETRN: A Heavy Ion/Nucleon Transport Code for Space Radiations.* NASA TP-3146, 1991.

16. Schimmerling, Walter: Ground-Based Measurements of Galactic Cosmic Ray Fragmentation in Shielding. Paper presented at the 28th Plenary Meeting of COSPAR (The Hague, The Netherlands), June 25–July 6, 1990.

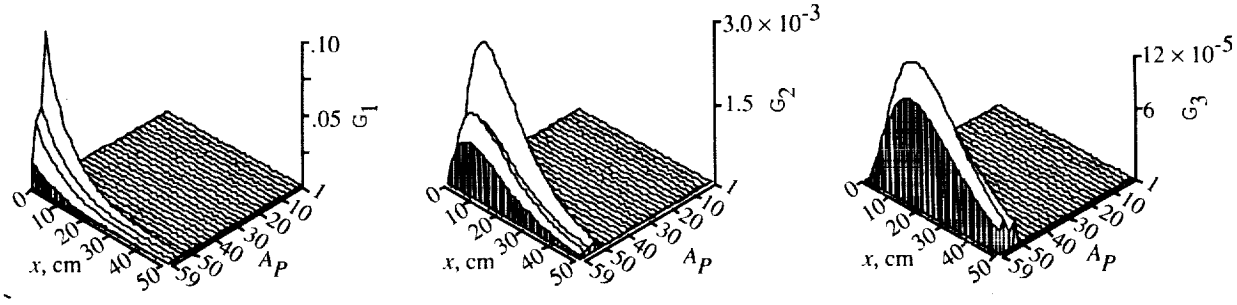

(a) First collision. (b) Second collision. (c) Third collision.

Figure 1. First three collision contributions to ^{52}Cr production.

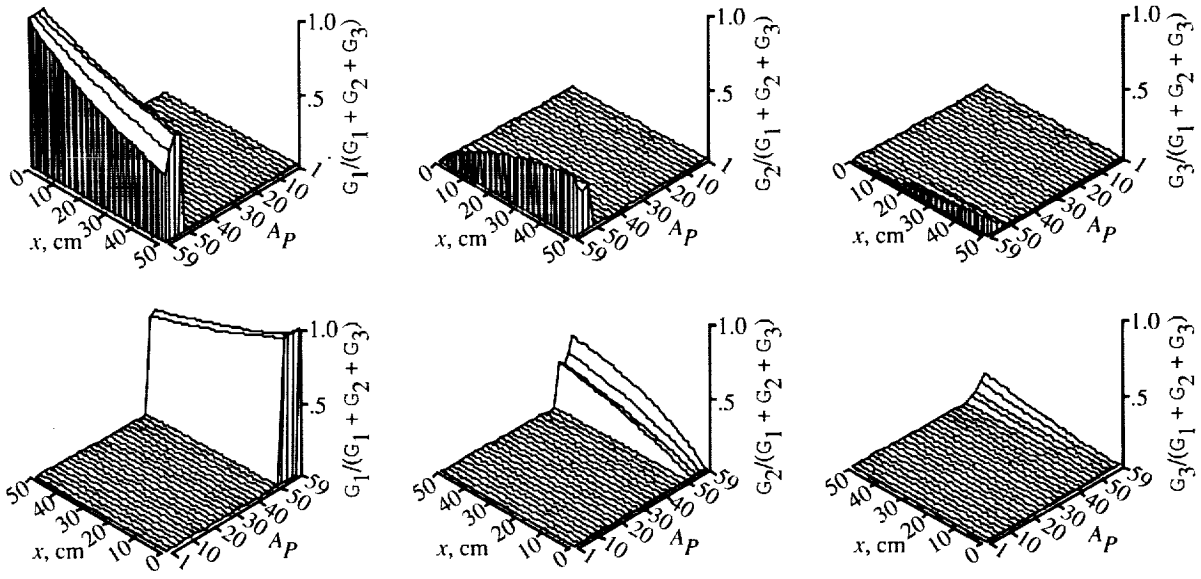

(a) First collision. (b) Second collision. (c) Third collision.

Figure 2. Fractional contribution to ^{52}Cr production from first three collision terms.

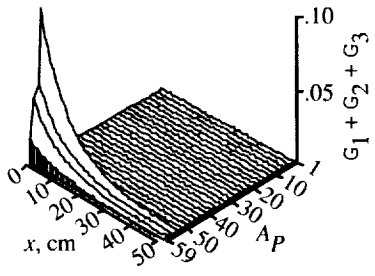

Figure 3. Total ^{52}Cr production from first three collisions.

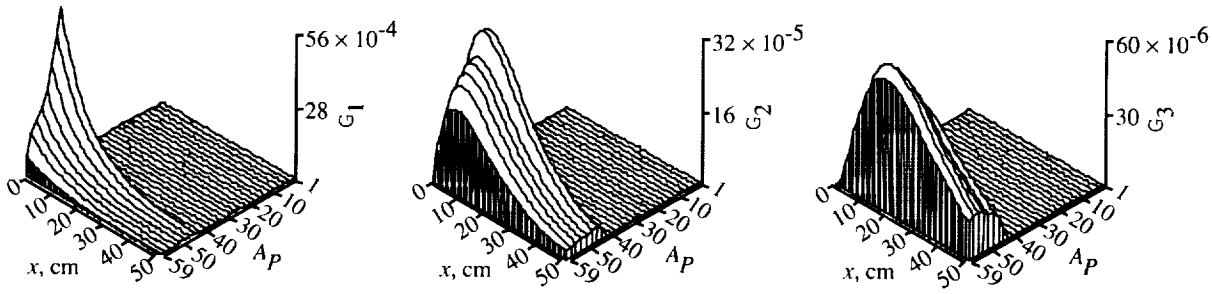

(a) First collision. (b) Second collision. (c) Third collision.

Figure 4. First three collision contributions to ^{40}Ar production.

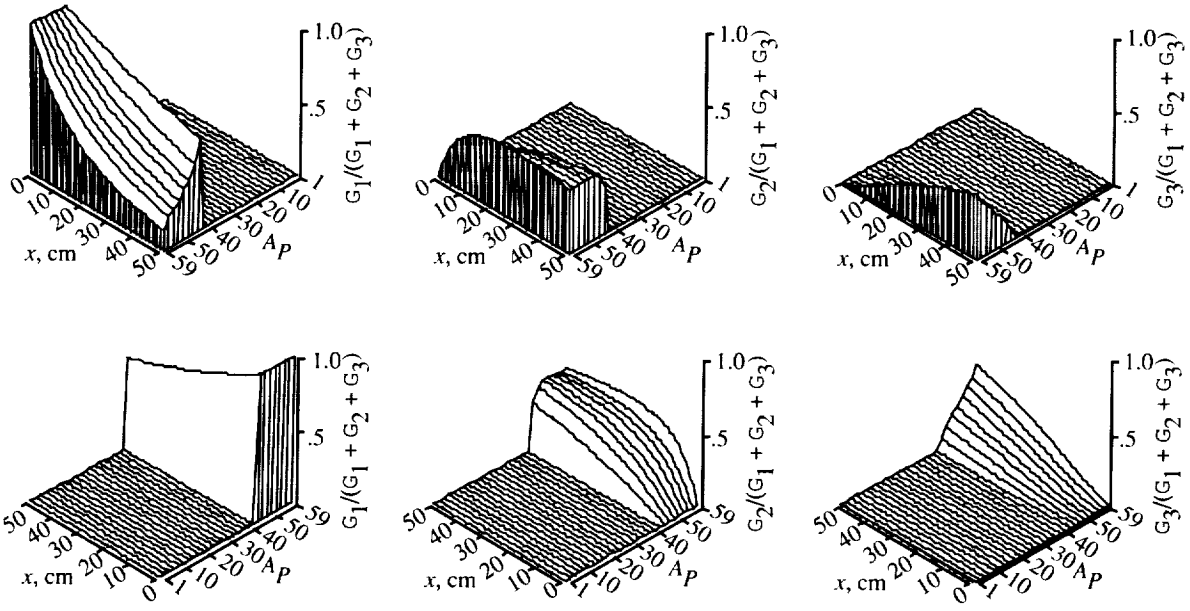

(a) First collision. (b) Second collision. (c) Third collision.

Figure 5. Fractional contribution to ^{40}Ar production from first three collision terms.

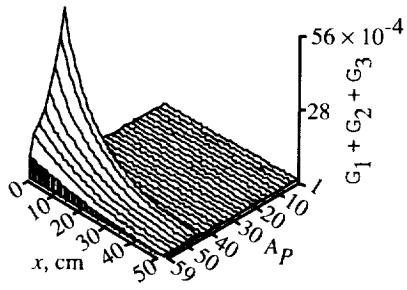

Figure 6. Total ^{40}Ar production from first three collisions.

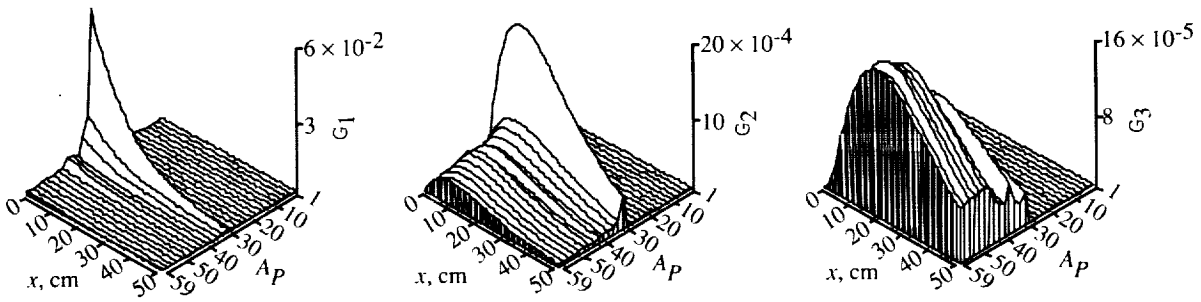

(a) First collision. (b) Second collision. (c) Third collision.

Figure 7. First three collision contributions to ^{28}Si production.

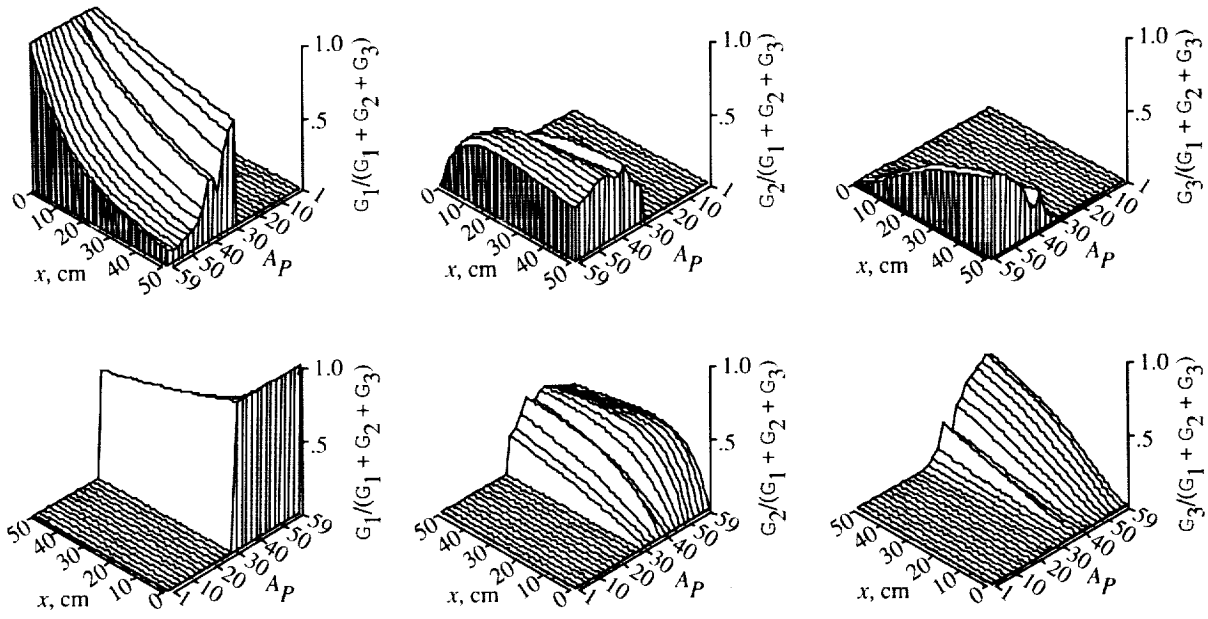

(a) First collision. (b) Second collision. (c) Third collision.

Figure 8. Fractional contribution to ^{28}Si production from first three collision terms.

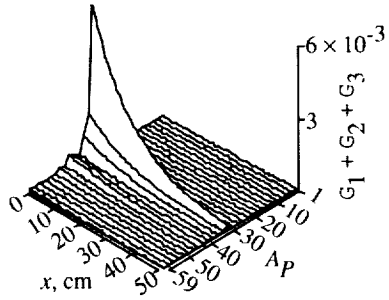

Figure 9. Total ^{28}Si production from first three collisions.

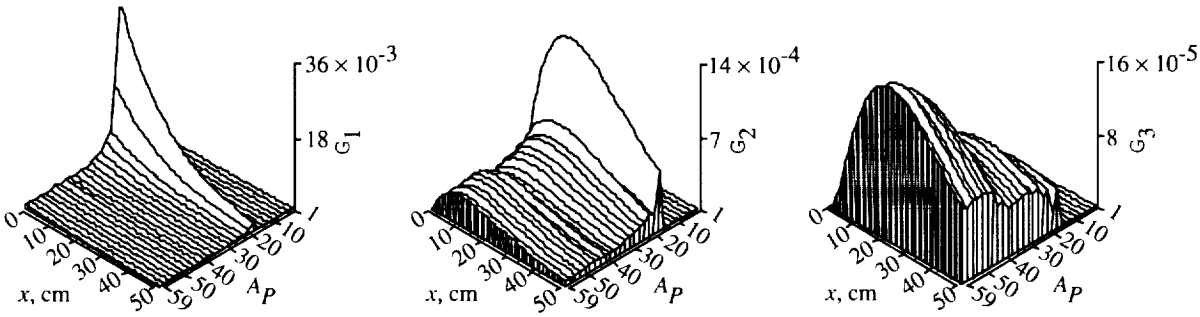

(a) First collision. (b) Second collision. (c) Third collision.

Figure 10. First three collision contributions to ^{16}O production.

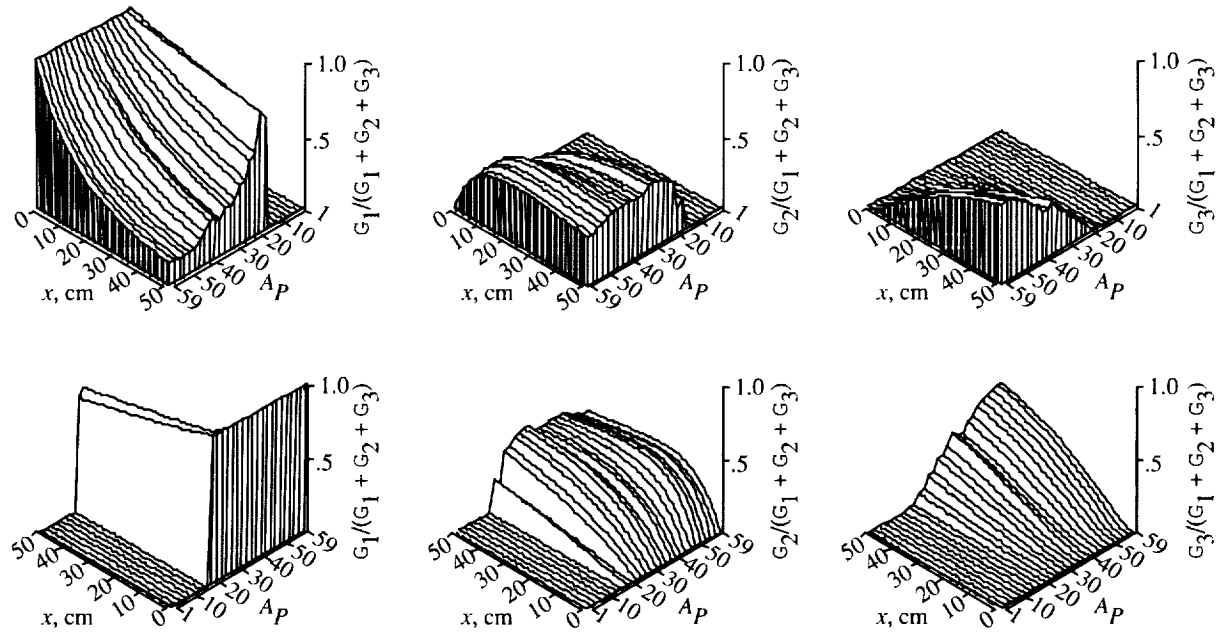

(a) First collision. (b) Second collision. (c) Third collision.

Figure 11. Fractional contribution to ^{16}O production from first three collision terms.

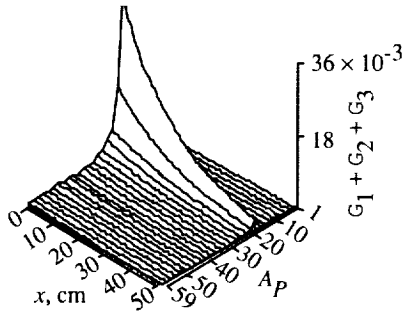

Figure 12. Total ^{16}O production from first three collisions.

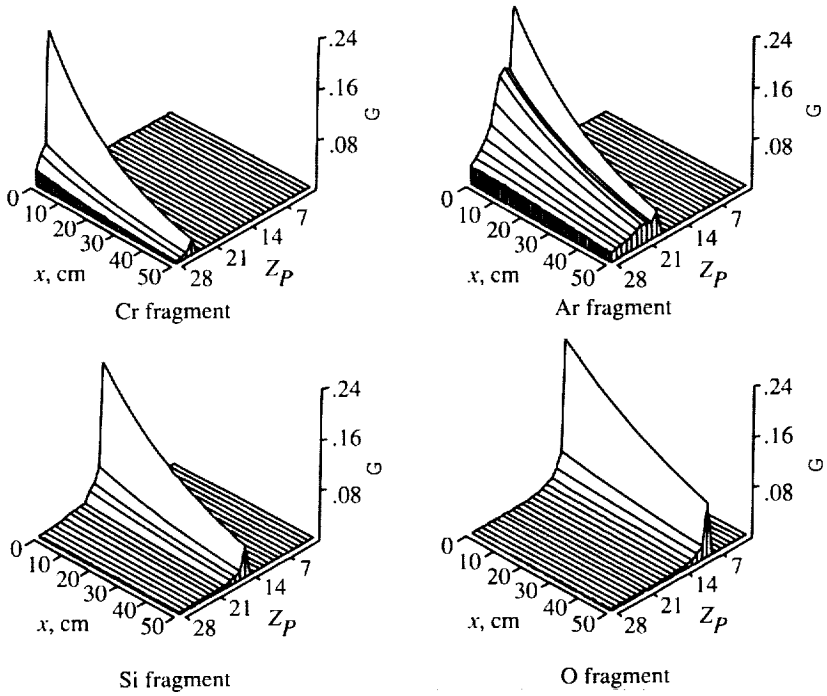

Figure 13. Total production of specific ions from various projectiles.

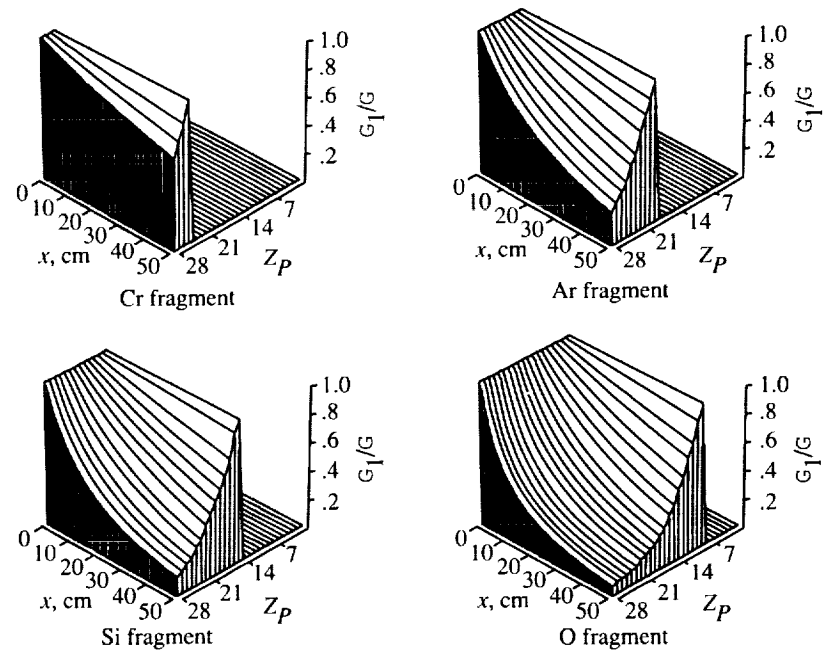

Figure 14. Fraction contribution of first collision term of specific elements.

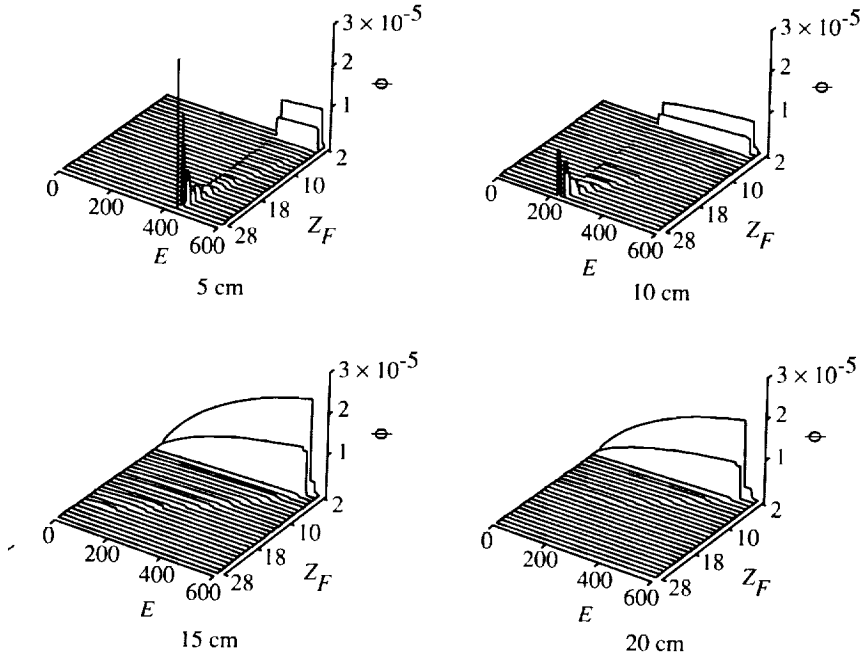

Figure 15. Composition of a 535 MeV/nucleon iron beam in a water column.

REPORT DOCUMENTATION PAGE

Form Approved
OMB No. 0704-0188

1. AGENCY USE ONLY *(Leave blank)*	2. REPORT DATE	3. REPORT TYPE AND DATES COVERED
	March 1993	Technical Paper

4. TITLE AND SUBTITLE
Green's Function Methods in Heavy Ion Shielding

5. FUNDING NUMBERS
WU 593-42-21-01

6. AUTHOR(S)
John W. Wilson, Robert C. Costen, Judy L. Shinn, and Francis F. Badavi

7. PERFORMING ORGANIZATION NAME(S) AND ADDRESS(ES)
NASA Langley Research Center
Hampton, VA 23681-0001

8. PERFORMING ORGANIZATION REPORT NUMBER
L-17184

9. SPONSORING/MONITORING AGENCY NAME(S) AND ADDRESS(ES)
National Aeronautics and Space Administration
Washington, DC 20546-0001

10. SPONSORING/MONITORING AGENCY REPORT NUMBER
NASA TP-3311

11. SUPPLEMENTARY NOTES
Wilson, Costen, and Shinn: Langley Research Center, Hampton, Virginia; Badavi: Christopher Newport University, Newport News, Virginia.

12a. DISTRIBUTION/AVAILABILITY STATEMENT
Unclassified - Unlimited

Subject Category 73

12b. DISTRIBUTION CODE

13. ABSTRACT *(Maximum 200 words)*
An analytic solution to the heavy ion transport equation in terms of Green's function is used to generate a highly efficient computer code for space applications. The efficiency of the computer code is accomplished by a nonperturbative technique extending Green's function over the solution domain. The computer code can also be applied to accelerator boundary conditions to allow code validation in laboratory experiments.

14. SUBJECT TERMS
Heavy ion transport; Green's function; Galactic cosmic rays

15. NUMBER OF PAGES
18

16. PRICE CODE
A03

17. SECURITY CLASSIFICATION OF REPORT	18. SECURITY CLASSIFICATION OF THIS PAGE	19. SECURITY CLASSIFICATION OF ABSTRACT	20. LIMITATION OF ABSTRACT
Unclassified	Unclassified		

NSN 7540-01-280-5500

Standard Form 298(Rev. 2-89)
Prescribed by ANSI Std. Z39-18
298-102

NASA-Langley, 1993